Alamandine abrogates neutrophil degranulation in atherosclerotic mice

Mach, François

How to cite

MACH, François. Alamandine abrogates neutrophil degranulation in atherosclerotic mice. In: European Journal of Clinical Investigation, 2017, vol. 47, n° 2, p. 117–128. doi: 10.1111/eci.12708

This publication URL: https://archive-ouverte.unige.ch/unige:112245
Publication DOI: 10.1111/eci.12708

DOI: 10.1111/eci.12708

ORIGINAL ARTICLE

Alamandine abrogates neutrophil degranulation in atherosclerotic mice

Analina R. Da Silva[*], Sébastien Lenglet[*], Federico Carbone[†], Fabienne Burger[*], Aline Roth[*], Luca Liberale[†], Aldo Bonaventura[†], Franco Dallegri[†,‡], Nikolaos Stergiopulos[§], Robson A. S. Santos[¶], François Mach[*], Rodrigo A. Fraga-Silva[§,a] and Fabrizio Montecucco[†,‡,**,a]

[*]Division of Cardiology, Department of Medical Specialties, Foundation for Medical Researches, University of Geneva, Geneva, Switzerland, [†]First Clinic of Internal Medicine, Department of Internal Medicine, University of Genoa School of Medicine, Genoa, Italy, [‡]IRCCS AOU San Martino – IST, Genoa, Italy, [§]Institute of Bioengineering, Ecole Polytechnique Fédérale de Lausanne, Lausanne, Switzerland, [¶]Department of Physiology and Biophysics, Federal University of Minas Gerais, Belo Horizonte, Minas Gerais, Brazil, [**]Centre of Excellence for Biomedical Research (CEBR), University of Genoa, Genoa, Italy

ABSTRACT

Background Neutrophil-mediated inflammation was recently identified as an active contributor to athero-progression. Therapeutic strategies inhibiting neutrophil degranulation or recruitment were hypothesized to positively impact on plaque vulnerability. In this study, we investigated whether treatment with the recently discovered agonist of the Mas-related G-coupled receptor type D (MrgD) alamandine would impact on neutrophil degranulation *in vivo* and *in vitro*.

Materials and methods Fifteen-week-old ApoE$^{-/-}$ mice were fed with a Western-type diet for an additional 11 weeks. After the first 2 weeks of diet, mice were surgically implanted with a carotid 'cast' device that alters the blood shear stress and induces different carotid plaque phenotypes. During the last 4 weeks before euthanasia, mice were randomly assigned to subcutaneously receive vehicle (NaCl 0·15 M) or alamandine (24 μg/kg/h) by micropump. For *in vitro* experiments, neutrophils were obtained after thioglycollate intraperitoneal injection in ApoE$^{-/-}$ mice.

Results Treatment with alamandine was well-tolerated, but failed to affect lipid, macrophage, neutrophil or collagen content within carotid and aortic root plaques. Also, treatment with alamandine did not affect Th-cell polarization in lymphoid organs. Conversely, alamandine administration was associated with a reduction in serum levels of neutrophil granule enzymes, such as MMP-9 and MPO as well as MMP-9 content within aortic root plaques. *In vitro*, preincubation with alamandine dose-dependently abrogated PMA-induced neutrophil degranulation of MMP-9 and MPO.

Conclusion These results suggest that treatment with the MrgD agonist alamandine led to a reduced release of neutrophil granule products, potentially interfering with pro-atherosclerotic neutrophil activation.

Keywords Atherosclerosis, Mas receptor, neutrophils.

Eur J Clin Invest 2017; 47 (2): 117–128

Introduction

Emerging evidence suggests that neutrophil activation plays a pathophysiological role in atherogenesis and its acute complications [1,2]. Animal models of both early and advanced phases of the disease demonstrated that neutrophils infiltrate atherosclerotic plaques [3,4]. Subsequently, neutrophil degranulation (both intraplaque and in the systemic circulation) was associated with atherosclerotic plaque vulnerability [5]. In human beings, higher intraplaque neutrophil content was shown in symptomatic as compared with asymptomatic carotid plaques [6]. Accordingly, high plasmatic and arterial levels of the neutrophil granule product myeloperoxidase were found in human and mouse cerebral aneurisms, a condition favouring haemorrhagic stroke [7]. Other neutrophil proteinases, such as matrix metalloproteinase (MMP)-8 and MMP-9, were also positively associated with the atherosclerotic risk [8,9], suggesting that these cells are an important source of degrading

[a]These authors contributed equally as last author to this work.

enzymes that actively cause damage in chronic vascular diseases including aneurysm. The renin–angiotensin system (RAS) was recently identified as a regulator of neutrophil-mediated processes in aneurysm formation and atherosclerotic plaques. In particular, in both humans and mice, neutrophils were shown to infiltrate the aortic intima and release MMP-9 in response to angiotensin (Ang) II stimulation [10]. On the other hand, treatment with the vasoactive peptide Ang-(1-7), an agonist of the Mas receptor, led to reduced atherosclerotic vulnerability and decreased neutrophil and MMP-9 intraplaque content [11]. These studies clearly support RAS as a potent regulator of deleterious pro-atherosclerotic activities of neutrophils [12]. During studies of newly discovered and more selective agonists of the Mas-related G-coupled receptor type D (MrgD), the peptide alamandine was recently identified as being generated by catalysis of Ang A via ACE2 or directly by aspartate decarboxylation from Ang-(1-7) [13]. In this study, we hypothesized that this endogenous peptide might actively interfere with neutrophil-mediated pathophysiological processes in atherogenesis. Therefore, we tested whether treatment with alamandine affects neutrophils as well as other inflammatory mediators in a mouse model of carotid atherogenesis ($ApoE^{-/-}$ mice implanted with a carotid 'cast' device). This model of shear stress-induced atherogenesis was previously shown to determine different carotid plaque phenotypes within carotids that could somehow mimic high heterogeneity of human lesions [14]. During further tests, we verified the role of alamandine in the *in vitro* degranulation of neutrophils isolated from $ApoE^{-/-}$ mice.

Materials and methods

Mouse model of atherogenesis and treatment

Apolipoprotein E-deficient mice ($ApoE^{-/-}$) in a C57BL/6J background were purchased from Jackson Laboratories (Les Oncins, France). The 15-week-old animals were transferred to receive a Western-type diet consisting of 15% (wt/wt) cocoa butter and 0·25% (wt/wt) cholesterol (Diet W; AbDiets, Lage, Germany) for an additional 11 weeks. After the first 2 weeks of Western diet, the shear stress in the right common carotid artery was altered by the surgical placement of a 'cast' device, as previously described [3,15,16]. The device induced low shear stress (LSS) in the carotid region upstream of the blood flow and oscillatory shear stress region (OSS) in the region downstream from the cast. The LSS and OSS carotid portions were characterized by the formation of atherosclerotic plaques that were collected at mouse euthanasia (9 weeks after surgery). At week 6 after cast implantation, $ApoE^{-/-}$ mice were anaesthetized using inhaled isoflurane and an incision in the midscapular region was made, through which a mini osmotic pump (Alzet model 2004; Johnson & Johnson, New Brunswick, NJ, USA) was inserted for subcutaneous drug administration. This took place during the last 4 weeks before euthanasia (from week 6 to week 9 of cast implantation).

Mice were randomly assigned to subcutaneously receive vehicle (NaCl 0·15 M) or alamandine (24 μg/kg/h; purchased from Phoenix Pharmaceuticals, Inc., Burlingame, CA, USA; cat. # 002-10). Animals were sacrificed under anaesthesia (ketamine and xylazine, 100 and 15 mg/kg, respectively) followed by blood sampling via cardiac puncture and cardiac perfusion of phosphate-buffered saline. This animal study was approved by the local ethics committee and Swiss authorities and conformed to the 'position of the American Heart Association on Research Animal Use'.

Atherosclerotic plaque processing and immunohistochemistry

Mouse carotid artery was macroscopically cut into three portions: the region upstream of the cast device (LSS), the region of the cast device [characterized by high shear stress (HSS)] and the region downstream of the cast (OSS). The obtained portions were immediately frozen in OCT. As previously described [14,15], no plaques were detected in HSS regions (data not shown). Mouse aortic sinuses as well as LSS and OSS carotid plaques were serially cut into 5-μm transversal sections. Five sections from mouse aortic roots and eleven sections from LSS and OSS carotid plaques were fixed in acetone and immunostained with specific antibodies: anti-mouse CD68 (macrophages; ABD Serotec, Dusseldorf, Germany), anti-mouse Ly-6G (neutrophils; BD Pharmingen™, San Jose, CA, USA) and anti-mouse MMP-9 (R&D Systems Inc, Minneapolis, MN, USA). Quantifications were performed using the METAMORPH software (Nashville, TN, USA). Results for other parameters were calculated as percentages of stained area over total lesion area or a number of infiltrating cells per mm^2 of lesion area [3,14,16].

Oil Red O staining for lipid content

Five sections of mouse aortic sinus and eleven sections of LSS and OSS carotid plaques were stained with Oil Red O, as previously described [14]. Sections of plaques were counterstained with Mayer's hemalun and rinsed in distilled water. Quantifications were performed using the METAMORPH software. Data were calculated as percentages of stained area on total lesion area.

Sirius red staining for collagen content

Five sections of mouse aortic sinus and eleven sections of LSS and OSS carotid plaques were rinsed with water and incubated with 0·1% Sirius red (Sigma Chemical Co, St Louis, MO, USA) in saturated picric acid for 90 min. Sections were rinsed twice with 0·01 N HCl for 1 min and then immersed in water. After dehydration with ethanol for 30 s and cover slipping, the sections were photographed with identical exposure settings

Table 1 Mouse primers and probes used for real-time PCR

Gene	Function	Nucleotide sequence	Size (bp)	Accession number
Cd4	Fw	5′-AGATCACAGTCTTCACCTGGAAGTT-3′	125	NM_013488
	Rv	5′-TGCCCCTTTTTTGGAATCAA-3′		
	Probe	5′-TTAATTAGAGGAGGTTCGCC-3′		
Cxcl1	Fw	5′-CATAGCCACACTCAAGAATGGT-3′	60	NM_008176
	Rv	5′-TGAACCAAGGGAGCTTCAG-3′		
	Probe	5′-CGCGAGGCTTGCCTTGACC-3′		
Cxcl2	Fw	5′-AGTGAACTGCGCTGTCAATG-3′	126	NM_009140
	Rv	5′-GCCCTTGAGAGTGGCTATGA-3′		
	Probe	5′-AAGACCCTGCCAAGGGTTGACTTC-3′		
Foxp3	Fw	5′-GGCCCTTCTCCAGGACAGA-3′	112	NM_054039
	Rv	5′-GCTGATCATGGCTGGGTTGT-3′		
	Probe	5′-ACTTCATGCATCAGCTCTCCACTGTGGAT-3′		
Gata3	Fw	5′-CAGAACCGGCCCCTTATCA-3′	115	NM_008091
	Rv	5′-CATTAGCGTTCCTCCTCCAGA-3′		
	Probe	5′-CGAAGGCTGTCGGCA-3′		
Havcr2 (Tim3)	Fw	5′-GCCGGTGGACCTCAGTTTC-3′	69	NM_134250
	Rv	5′-TGGGAGCCAGCACAGATCA-3′		
	Probe	5′-ACAGCTGCCTGCCCAGTGCCC-3′		
Hprt	Fw	5′-GACCGGTCCCGTCATGC-3′	66	NM_013556
	Rv	5′-TCATAACCTGGTTCATCATCGC-3′		
	Probe	5′-ACCCGCAGTCCCAGCGTCGTG-3′		
Ifng	Fw	5′-TGAGTATTGCCAAGTTTGAGGTCA-3′	77	NM_008337
	Rv	5′-GTGGACCACTCGGATGAGCT-3′		
	Probe	5′-CCACAGGTCCAGCGCCAAGCA-3′		
Il4	Fw	5′- CAACGAAGAACACCACAGAGAG -3′	89	NM_021283
	Rv	5′- GCATGGAGTTTTCCCATGTT -3′		
	Probe	5′-AGCTCGTCTGTAGGGCTTCCAAGGT-3′		
Il10	Fw	5′-TTTGAATTCCCTGGGTGAGAA-3′	73	NM_010548
	Rv	5′-ACAGGGGAGAAATCGATGACA-3′		
	Probe	5′-TGAAGACCCTCAGGATGCGGCTG-3′		
Il17a	Fw	5′-CTGTGATCTGGGAAGCTCAGT-3′	124	NM_010552
	Rv	5′-CTCTCAGGCTCCCTCTTCAG-3′		
	Probe	5′-CTGTGTCAATGCGGAGGGAAAG-3′		
Mmp8	Fw	5′-GCATTCAGACAATCTATGGACCT-3′	101	NM_008611
	Rv	5′-GGTAGTAGCATCAAATCTCAGGTG-3′		
	Probe	5′-TCAGACAACCCCATCCAACCTACTG-3′		

Table 1 *Continued*

Gene	Function	Nucleotide sequence	Size (bp)	Accession number
Mmp9	Fw	5′-GTATCTGTATGGTCGTGGCTCTAA-3′	91	NM_013599
	Rv	5′-ACACATAGTGGGAGGTGCTGT-3′		
	Probe	5′-CTCCAGCCACCACCACAACTGAA-3′		
Mpo	Fw	5′-ACGTGATGGTGATCGGTTTT-3′	117	NM_010824
	Rv	5′-GTGGTGATGCCAGTGTTGTC-3′		
	Probe	5′-CAGGCGTGTTCAGTAAACAGCAGAGA-3′		
Rorc	Fw	5′-AGAAGACCCACACCTCACAAA-3′	89	NM_011281
	Rv	5′-ACAGGTGATAACCCCGTAGTG-3′		
	Probe	5′-CCCTTGCAAGATCTGTGGGGACA-3′		
Mmp10	Fw	5′-CTCCAGCCACCACCACAACTGAA-3′	132	NM_019471
	Rv	5′-ATGCTTGGGTGGCCTTGT-3′		
	Probe	5′-CTGTCTGTATGGAGCCACTAGCCATCCT-3′		
Mmp12	Fw	5′-AAAGACTGGTTCTTCTGGTGGA-3′	91	NM_008605
	Rv	5′-TACCAGATGGGATGCTTGG-3′		
	Probe	5′-CTTCCTGGGAGTCCAGCCACCA-3′		
Mmp3	Fw	5′-TGCAGTTGGAGAACATGGAG-3′	141	NM_010809
	Rv	5′-GTACCAGTGACATCCTCTGTCC-3′		
	Probe	5′-TTTTGATGGGCCTGGAACAGTCTTG-3′		
Tnf	Fw	5′-GTCCCCAAAGGGATGAGAAG-3′	134	NM_013693
	Rv	5′-CACTTGGTGGTTTGCTACGA-3′		
	Probe	5′-CCCAAATGGCCTCCCTCTCATC-3′		
MrgD	Fw	5′-AGGAGCAGGAATGAACTCCA-3′	84	NM_203490
	Rv	5′-TTGACAGCAGCCCAGCTCCAG-3′		
	Probe	5′-ATCCAGGTCACAAGGTCCAT-3′		

under ordinary polychromatic or polarized light microscopy. Total collagen content was evaluated under polychromatic light. Interstitial collagen subtypes were evaluated using polarized light illumination; under this condition, thicker type I collagen fibres appeared orange or red, whereas thinner type III collagen fibres were yellow or green [14]. Quantifications were performed with METAMORPH software. Data were calculated as percentages of stained area over total lesion area.

Measurements of serum inflammatory molecule levels

Colorimetric enzyme-linked immunosorbent assay (ELISA) kits to measure serum CXCL1, CCL2, pro-matrix metalloproteinase (MMP)-9, myeloperoxidase (MPO) and tissue inhibitor of metalloproteinase-1 (TIMP-1) levels (all from R&D Systems), and serum MMP-8 levels (Uscn Life Science Inc., Hubei, China) were used following manufacturer's instructions. The limit of detection was 15·6 pg/mL for CXCL1, 3·9 pg/mL for CCL2, 31·25 pg/mL for pro-MMP-9, 250 pg/mL for MPO, 37·5 pg/mL for TIMP-1 and 312·5 pg/mL for MMP-8. Mean intra- and interassay coefficients of variation (CV) were below 6%.

PCR

Total RNA was extracted from mouse neutrophils and atherosclerotic aorta with Trizol reagent (Ambion, Carlsbad, CA, USA), following the manufacturer's instructions. The concentration and purity of RNA were determined by spectrophotometry analysis, and cDNA was prepared from 1000 ng total RNA using the ImProm-II Reverse Transcription kit

(Promega Corporation, Madison, WI, USA), as suggested by the manufacturer. As a negative control, reverse transcription experiments were performed by omitting the reverse transcriptase enzyme from the reactions (RT-). PCR was performed using primer pairs specific for mouse Mas-related GPR (Mrg-prd) based on the nucleotide sequences available in GenBank (forward primer: 5′-aggagcaggaatgaactcca-3′ and reverse primer: 5′-ataccagatggggaaaagcac-3′). The house-keeping gene hypoxanthine-guanine phosphoribosyl transferase (Hprt) was used as a positive control (forward primer: 5′-tggatacaggcca-gactttgtt-3′ and reverse primer: 5′- gataagcgacaatctaccagagg-3′). The PCR products were separated by electrophoresis on 2% agarose gel stained with SYBR Safe (Invitrogen Corporation, Carlsbad, CA, USA) and viewed under UV light.

Table 2 Laboratory parameters of adult ApoE$^{-/-}$ mice at sacrifice

Mouse characteristics	Vehicle-treated mice (n = 8)	Alamandine-treated mice (n = 9)	P-value
Serum metabolism and lipids			
Total cholesterol, mM	25·91 (16·43–38·75)	25·62 (21·35–36·62)	0·738
LDL cholesterol, mM	12·02 (8·24–15·78)	15·03 (6·10–18·10)	0·738
HDL cholesterol, mM	0·80 (0·66–11·29)	0·96 (0·78–1·09)	0·908
Triglycerides, mM	5·51 (3·22–5·98)	5·15 (4·58–6·07)	1·000
Free fatty acids, mM	19·89 (11·62–4·07)	20·49 (15·96–26·27)	0·655
Glucose, mM	1·54 (0·67–4·07)	1·42 (0·93–2·50)	1·000
Inflammation			
CCL2, pg/mL	63·08 (51·12–77·05)	67·11 (37·77–84·39)	0·931
CXCL1, pg/mL	58·28 (49·15–109·84)	61·86 (59·46–84·56)	0·436

Data are expressed as median (interquartile range).
P-value calculated according to Mann–Whitney U-test.

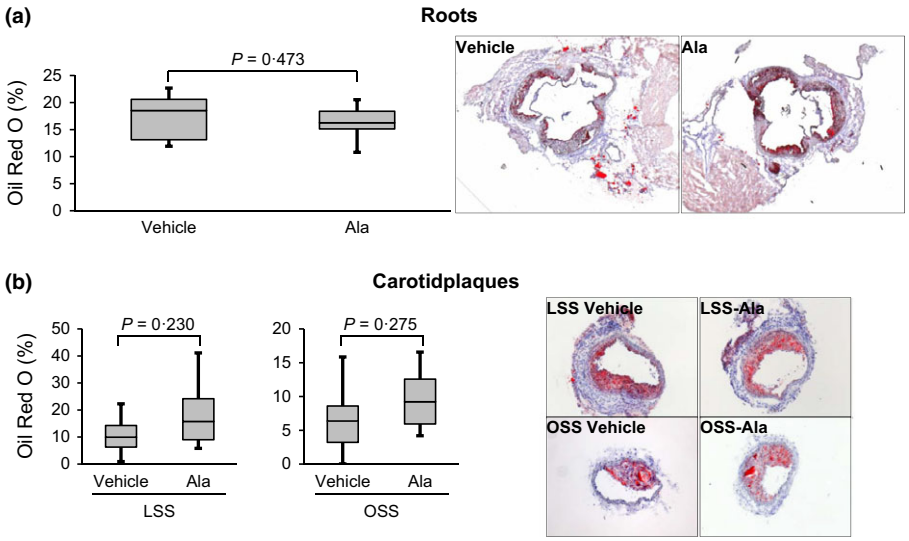

Figure 1 Treatment with alamandine does not affect intraplaque lipids. ApoE$^{-/-}$ mice treated with vehicle (NaCl 0·15 M) or alamandine (Ala), 24 μg/kg/h for 4 weeks before euthanasia. Data are expressed as median (interquartile range), n = 8–9 per group. (a) Quantification and representative microphotographs (Oil Red O staining) of lipid content in aortic root plaques. (b) Quantification and representative microphotographs of lipid content in carotid plaques under low shear stress (LSS) or oscillatory shear stress (OSS).

Real-time RT-PCR

Total mRNA was isolated with Tri-reagent (Molecular Research Center, Inc., (MRC), Cincinnati, OH, USA) from lymph nodes, spleen and abdominal aortas of ApoE$^{-/-}$ mice. Reverse transcription was performed using the ImProm-II Reverse Transcription System (Promega) according to the manufacturer's instructions. Real-time PCR (StepOne Plus; Applied Biosystems, Waltham, MA, USA) was performed with the ABsolute™ QPCR Mix (ABgene by Thermo Scientific, Hudson, NH, USA).

Specific primers and probes (Table 1) were used to determine the mRNA expression of MrgD, neutrophil chemoattractants (Cxcl1, Cxcl2, Tnf), enzymes and proteases (Mpo, Mmp-3, Mmp-8, Mmp-9, Mmp-10, Mmp-12) and markers of different T helper (Th) CD4$^+$ lymphocyte subsets (Th1: Tim3, Ifng; Th2: Gata-3, Il4; Treg: Foxp3, Il10; Th17: Rorc, Il17) and Hprt (reference gene) [17]. The fold change of mRNA levels was calculated by the comparative C_t method. The resultant C_t values were first normalized to the internal control. This was achieved by calculating a delta C_t (ΔC_t) by subtracting the internal control C_t values from the Hprt C_t value. A delta delta C_t ($\Delta\Delta C_t$) was calculated by subtracting the designated control ΔC_t value from the other ΔC_t values. The $\Delta\Delta C_t$ was then plotted as a relative fold change with the following formula: $2-\Delta\Delta C_t$.

Mouse neutrophil degranulation assay

Neutrophils were obtained from 11-week-old ApoE$^{-/-}$ mice under a normal chow diet after an intraperitoneal injection of 4% thioglycollate solution, as previously described [17]. The peritoneal lavage fluids of mice (n = 14) were used. Neutrophils were resuspended in culture medium (serum-free RPMI 1640 medium containing 25 mM Hepes) and cultured at 5×10^5 cells per well. The cells were pre-incubated for 60 min in the presence or absence of control medium or different doses (1×10^{-7} to 1×10^{-4} M) of alamandine. Then, a control medium or 10 ng/mL phorbol-12-myristate-13-acetate (PMA, positive control from Sigma-Aldrich, Buchs, Switzerland) was added for an additional 30 min at 37 °C in a humidified atmosphere of 5% CO_2 in polystyrene plates without washing. The cell supernatants were collected to be tested for degranulation of pro-MMP-9 and MPO. Levels of pro-MMP-9 and MPO in mouse neutrophil supernatants were assessed by the same ELISA kits from R&D systems that were used to detect these molecules in mouse serum.

Statistical analysis

Statistical analyses were performed with IBM SPSS STATISTICS for Windows, Version 23.0 (IBM Corp., Armonk, NY, USA). Continuous variables are presented as median [interquartile range (IQR)]. Two group comparisons were then performed using a two-tailed t-test (paired and unpaired) or nonparametric Mann–Whitney U-test when the normality assumption of variable distribution was violated. Finally, one-way ANOVA was used for multiple group comparison. A two-sided P-value < 0·05 was considered statistically significant.

Table 3 T helper cell polarization in lymphatic tissues

Marker (mRNA fold increase)	Vehicle-treated mice (n = 8)	Alamandine-treated mice (n = 9)	P-value
Lymph nodes			
Cd4	1·09 (0·78–1·19)	0·99 (0·77–1·52)	0·862
Th1			
Tim3	1·00 (0·79–1·16)	1·15 (1·01–1·53)	0·113
Ifnγ	0·97 (0·79–1·25)	1·01 (0·54–1·26)	0·869
Th2			
Gata3	0·99 (0·77–1·25)	0·87 (0·75–1·21)	0·798
Il4	1·00 (0·74–1·19)	1·16 (0·65–1·58)	0·469
Treg			
Foxp3	0·99 (0·74–1·14)	0·90 (0·78–1·13)	0·869
Il10	0·97 (0·85–1·10)	1·28 (0·95–1·60)	0·113
Th17			
Rorc	0·27 (0·16–1·37)	0·35 (0·06–1·72)	0·595
Il17	0·95 (0·74–1·30)	1·58 (0·72–3·49)	0·113
Spleen			
Cd4	0·96 (0·80–1·12)	1·08 (0·92–1·24)	0·315
Th1			
Tim3	1·00 (0·78–1·19)	0·97 (0·94–1·23)	0·362
Ifnγ	0·93 (0·80–1·26)	0·96 (0·70–1·23)	1·000
Th2			
Gata3	0·96 (0·77–1·13)	1·10 (0·92–1·20)	0·414
Il4	0·93 (0·75–1·42)	0·88 (0·68–1·06)	0·318
Treg			
Foxp3	0·94 (0·78–1·20)	1·01 (0·93–1·12)	0·654
Il10	0·99 (0·70–1·33)	1·15 (0·90–2·33)	0·197
Th17			
Rorc	0·78 (0·49–1·36)	1·22 (0·75–2·19)	0·315
Il17	0·83 (0·50–1·16)	1·05 (0·59–1·63)	0·721

Data are expressed as median (IQR).
P-value calculated according to Mann–Whitney U-test.

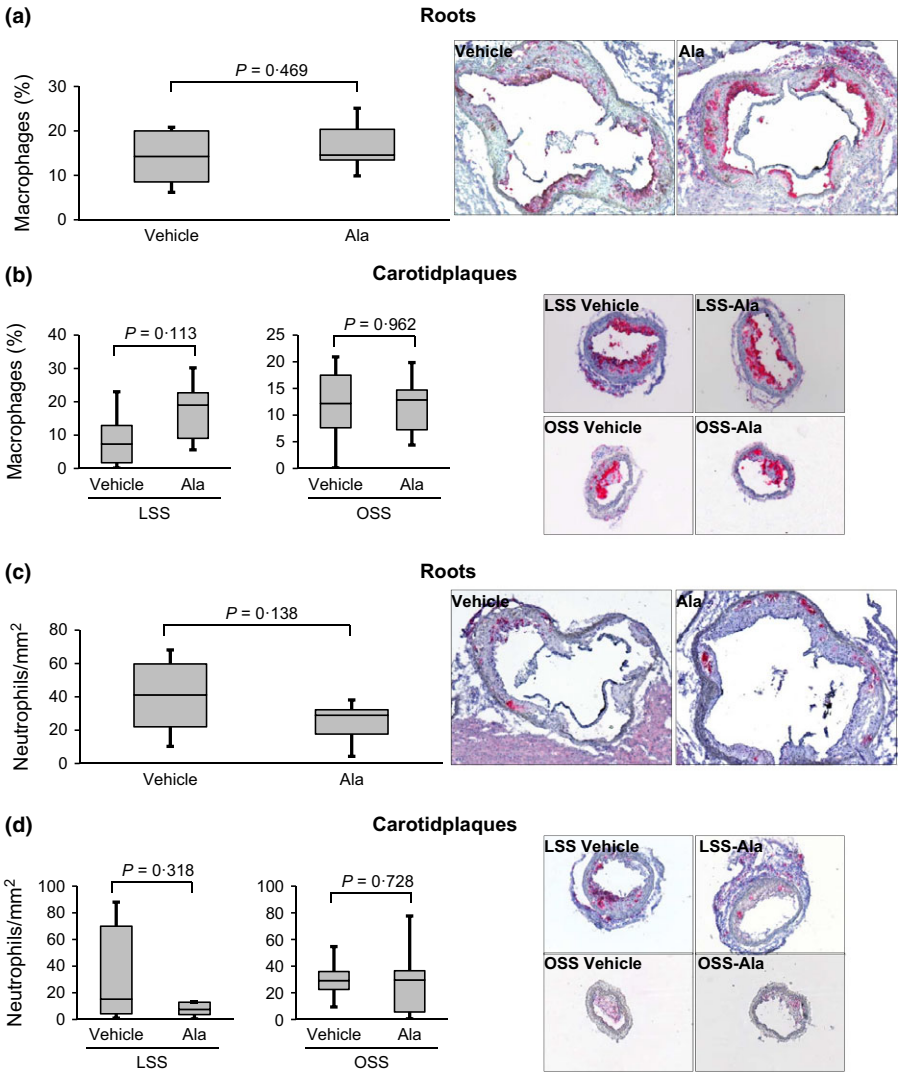

Figure 2 Treatment with alamandine does not affect intraplaque macrophage or neutrophil content. ApoE$^{-/-}$ mice treated with vehicle (NaCl 0·15 M) or alamandine (Ala), 24 μg/kg/h for 4 weeks before euthanasia. Data are expressed as median (interquartile range), n = 8–9 per group. (a) Quantification and representative microphotographs of macrophage content (CD68^{+} cells) in aortic root plaques. (b) Quantification and representative microphotographs of macrophage content in carotid plaques under LSS or OSS. (c) Quantification and representative microphotographs of neutrophil (Ly-6G^{+} cells) content in aortic root plaques. (d) Quantification and representative microphotographs of neutrophil content in carotid plaques under low shear stress (LSS) or oscillatory shear stress (OSS).

Results

Treatment with alamandine does not affect the lipid profile and intraplaque lipids in aortic root and carotid plaques

The potential effects of alamandine treatment on metabolic parameters were assessed at mouse euthanasia. Treatment with alamandine did not induce any significant change in the serum lipid profile, glucose or inflammatory chemokines (i.e. CCL2 and CXCL1) as compared with the control vehicle (Table 2). Accordingly, treatment with alamandine did not affect intraplaque lipid content in aortic root plaques or in carotid LSS and OSS atheroma as compared with the control vehicle (Fig. 1a,b).

Treatment with alamandine does not affect intraplaque macrophage or neutrophil content within atherosclerotic plaques

The potential effects of treatment with alamandine on inflammatory mechanisms regulating atherogenesis were investigated within lymphoid organs (i.e. lymph nodes and spleen) and atherosclerotic plaques. No difference on T-cell subsets (Th1/Th2/TregTh17) was observed within lymphoid organs between alamandine- and vehicle-treated mice (Table 3). Accordingly, treatment with alamandine was not associated with any change in total macrophage content within both aortic root and carotid LSS and OSS plaques (Fig. 2a,b). In addition, treatment with alamandine did not affect neutrophil intraplaque content as compared with the control vehicle (Fig. 2c,d). Finally, treatment

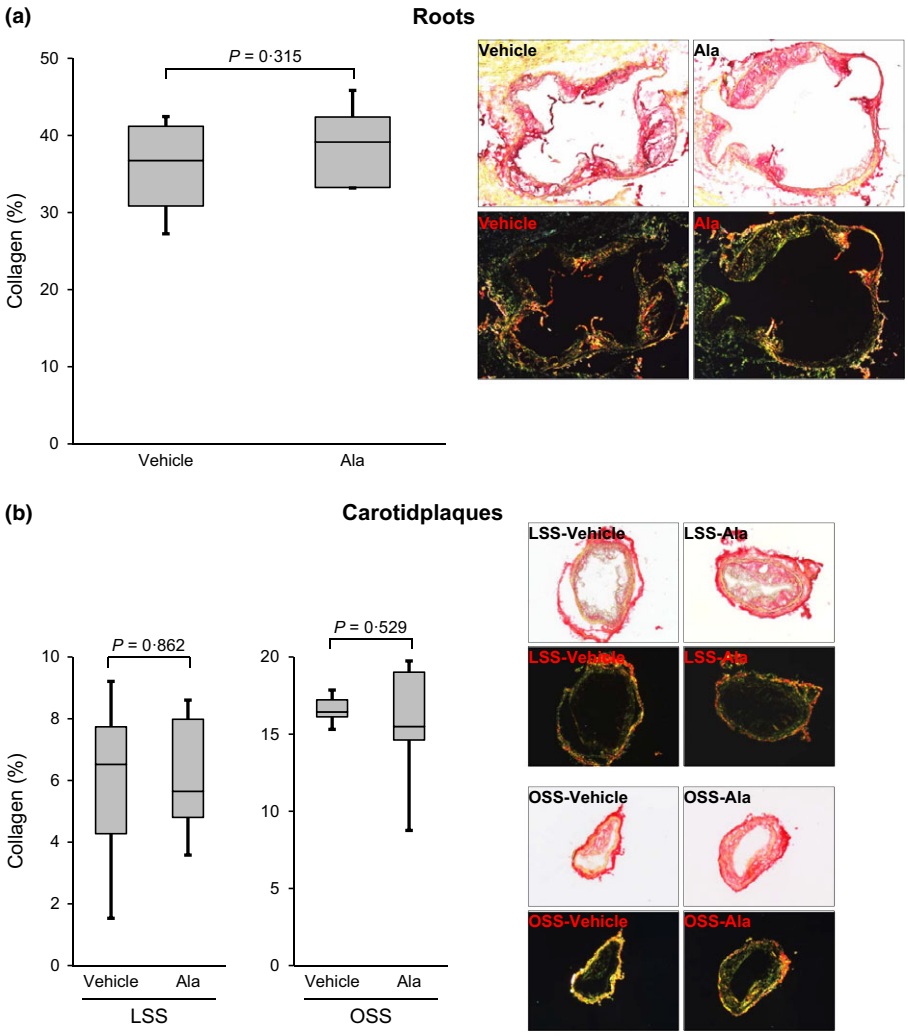

Figure 3 Treatment with alamandine does not affect intraplaque collagen content. (a, b) Quantification of collagen content and representative microphotographs of Sirius red-stained plaques from aortic roots (a) and carotids under low shear stress (LSS) or oscillatory shear stress (OSS) (b). Collagen specificity is shown under bright illumination without polarization (upper part) and under polarized light illumination (lower part). Data are expressed as median (interquartile range), n = 8–9 per group.

with alamandine was not associated with any modification of collagen content as compared with the control vehicle within both aortic root and carotid LSS and OSS plaques (Fig. 3a,b).

Treatment with alamandine is associated with a reduction in circulating and intraplaque levels of MMP-9

We first investigated whether MrgD (the alamandine receptor) was expressed in neutrophils isolated from ApoE$^{-/-}$ mice. The mRNA expression of Mrgprd was present in neutrophils isolated from ApoE$^{-/-}$ mouse donors in a comparable manner to the positive-control tissue (the aorta from an ApoE$^{-/-}$ mouse; Fig. 4a). The mRNA quality was confirmed by the expression of the housekeeping gene Hprt (Fig. 4b). Treatment with alamandine was associated *in vivo* with a reduction in circulating levels of some neutrophil granule products (i.e. MMP-9 and MPO) as compared with vehicle-treated mice (Table 4). Also, a nonsignificant (P = 0·093) reduction in MMP-8 serum levels was observed in alamandine-treated mice as compared with vehicle (Table 4). Reduction in these proteases and myeloperoxidase was not accompanied by any modification in TIMP-1 serum levels between the study groups (Table 4). Within mouse plaques, treatment with alamandine significantly reduced MMP-9 content in aortic roots, but not in carotid LSS and OSS portions (Fig. 5a,b). Accordingly, a significant reduction in MMP-9 mRNA expression was reported in aortas from atherosclerotic mice treated with alamandine as compared with vehicle-treated mice (Table 5). Importantly, no difference in mRNA levels of other MMPs, Mpo, Timp-1 as well as pro-atherosclerotic molecules (i.e. Cxcl1, Cxl2, Tnf) was noted between alamandine- and vehicle-treated mice (Table 5).

Pretreatment with different concentrations of alamandine was finally tested on PMA-induced degranulation of neutrophils isolated from ApoE$^{-/-}$ mice. Pre-incubation with 10^{-4} M alamandine abrogated neutrophil degranulation of both MMP-9 and MPO in response to PMA (Fig. 6a,b). The alamandine-mediated effect on degranulation was dose-dependent (Fig. 6a,b).

Both *in vivo* and *in vitro* experiments suggest that treatment with alamandine was associated with a beneficial reduction in the amount of proteases and MPO of potential neutrophil origin.

Discussion

The main finding of this study is that treatment with alamandine can reduce neutrophil degranulation *in vitro*. *In vivo*, treatment with comparable concentrations of alamandine was associated with abrogation of the same neutrophil granule enzymes in the systemic circulation and within aortic root plaques, but not in carotid arteries. The apparent discrepancy between plaques at different sites of atherosclerosis might reflect high heterogeneity of the lesions that was also described in human beings [14]. Among other ligands [such as Ang-(1-7)], alamandine was previously shown to activate MrgD-mediated anti-inflammatory pathways [13]. This receptor was shown to protect mice from both acute injury and chronic inflammatory injury. For instance, the genetic deletion of Mas receptor in C57BL/6 mice resulted in an increased inflammatory response to LPS injection, suggesting a potent anti-inflammatory role of this receptor in acute systemic inflammatory disorders [18]. In a neonatal rat model of chronic lung disease (CLD), treatment with agonists of the Mas receptor was associated with lower pulmonary influx of neutrophils, thus potentially reducing lung injury [19]. Confirming these results, a recent study using male Sprague-Dawley rats, Balb/c and C57Bl6/J mice with acute lung injury showed that antagonism of the Mas receptor with A779 was able to restore neutrophil infiltration within the lungs [20]. The modulation of neutrophil degranulation was also suggested as a promising therapeutic target against atherogenesis. Evidence from our research group supported an active role for neutrophil pro-inflammatory functions (i.e. degranulation) in plaque vulnerability [5,9]. Our *in vivo* experiments demonstrated that treatment with alamandine was associated with abrogation of neutrophil granule enzymes in both the systemic circulation and aortic root plaques. In particular, marked reductions in MMP-9 and MPO levels were observed in alamandine-treated mice as compared with the control vehicle. Importantly, we also observed a significant reduction in MMP-9 mRNA expression levels within atherosclerotic aortic tissues. These results might suggest that alamandine treatment could be associated with a reduced expression (and not only a release) of proteases in atherogenesis. Although MMP-9, MMP-8 and MPO might be released by other cell subsets (i.e. macrophages) [21–23], neutrophils still represent a major source of these toxic compounds within

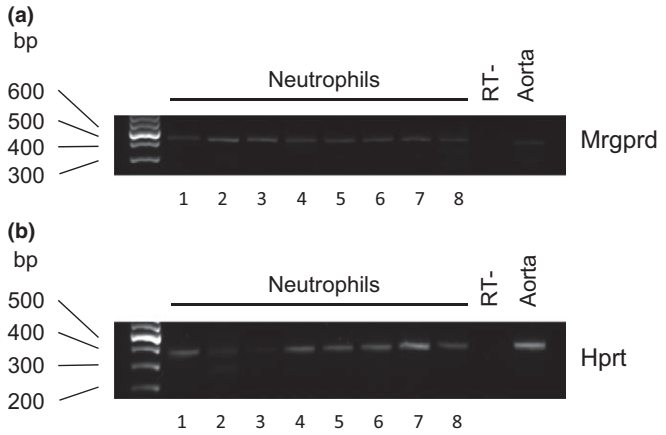

Figure 4 Mrgprd is expressed in mouse primary neutrophils. (a, b) Representative agarose gels of PCR products from mouse neutrophils (isolated from eight different ApoE$^{-/-}$ mouse donors 1–8) a positive control tissue (mouse atherosclerotic aorta) showing mRNA expression of (a) Mrgprd and (b) Hprt. A molecular weight size marker is shown on the left side of the agarose gel.

Table 4 Serum levels of proteases, MPO and TIMP-1 in ApoE$^{-/-}$ mice at sacrifice

Mouse characteristics	Vehicle-treated mice (n = 8)	Alamandine-treated mice (n = 9)	P-value
MMP-8, ng/mL	46·13 (37·29–52·25)	37·09 (30·34–41·94)	0·093
Pro-MMP-9, ng/mL	33·19 (24·94–112·82)	16·33 (11·55–25·87)	0·036
MPO, ng/mL	117·84 (91·78–127·70)	72·76 (61·10–91·02)	0·008
TIMP-1, ng/mL	1·03 (0·92–1·38)	1·27 (1·06–1·82)	0·197

Data are expressed as median (interquartile range).
P-value calculated according to Mann–Whitney *U*-test.

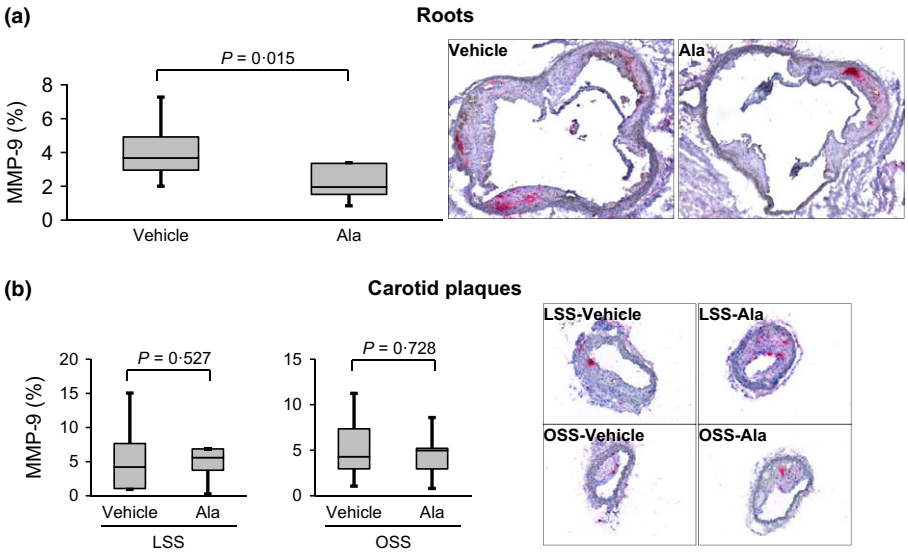

Figure 5 Treatment with alamandine reduces MMP-9 content in aortic root plaques. ApoE$^{-/-}$ mice treated with vehicle (NaCl 0·15 M) or alamandine (Ala), 24 μg/kg/h for 4 weeks before euthanasia. Data are expressed as median (interquartile range), n = 8–9 per group. (a) Quantification of MMP-9 content in aortic root plaques and representative microphotographs. (b) Quantification of MMP-9 content in carotid plaques under LSS or OSS and representative microphotographs.

Table 5 Inflammatory molecules and proteases in mouse aorta

Marker (mRNA fold increase)	Vehicle-treated mice (n = 8)	Alamandine-treated mice (n = 9)	*P*-value
Cxcl1	0·96 (0·42–1·57)	1·76 (0·60–2·17)	0·278
Cxcl2	0·88 (0·56–1·23)	1·08 (0·72–1·81)	0·410
Tnf-a	1·18 (0·54–1·26)	1·10 (0·35–1·85)	0·751
Mmp-3	0·93 (0·48–1·33)	0·71 (0·27–1·70)	0·761
Mmp-8	0·69 (0·29–1·73)	0·88 (0·62–1·45)	0·689
Mmp-9	0·81 (0·74–1·26)	0·70 (0·49–0·74)	0·029
Mmp-10	0·69 (0·55–1·80)	0·48 (0·18–1·32)	0·187
Mmp-12	0·91 (0·15–1·78)	0·60 (0·35–1·46)	0·932
Timp-1	1·04 (0·55–1·39)	1·42 (0·84–4·31)	0·165
Mpo	0·67 (0·56–1·44)	1·80 (0·62–6·72)	0·256

Data are expressed as median (IQR).
P-value calculated according to Mann–Whitney *U*-test.

mouse plaques [14], where their activity might degrade the protective collagen in the fibrous cap and increase the risk of plaque rupture. Although alamandine treatment was able to reduce neutrophil proteases, this benefit was not accompanied by any amelioration in the plaque structural stability. Intraplaque collagen content was similar in alamandine- and vehicle-treated mice. This apparent discrepancy might be explained by the fact that neutrophil-mediated injury is not the only one determinant of plaque vulnerability. By interfering with the RAS, alamandine might in principle affect mouse blood pressure or trigger adverse pro-atherosclerotic activities that counterbalance the benefits of neutrophil inhibition. Unfortunately, we were not able to assess all mouse hemodynamic and inflammatory parameters in this pilot study. However, this point must certainly be acknowledged as the main study limitation and deserves additional investigation with targeted monitoring equipment. To add information on other potential 'pleiotropic effects' of alamandine, we tested to verify whether this peptide was able to interfere with intraplaque macrophages and Th lymphocyte polarization in lymphoid organs. As no difference between groups was shown, we could speculate that alamandine treatment might selectively affect neutrophils without inducing a potential systemic immunosuppression. One of the main limitations of this study is represented by the fact that we were able to treat animals with a single dose of alamandine, instead of testing a dose–response curve as compared with placebo. Therefore, the lack of efficacy of alamandine treatment on coronary plaque composition deserves further investigations. In addition, a longitudinal study of the effects of alamandine on plaque composition also still needs to be studied. Therefore, this study has to be considered as 'pilot' investigation. Another study limitation is represented by the fact that the presence of the Mas-related G-coupled receptor type D on mouse neutrophils was demonstrated by PCR. Additional technical methods, such as binding assays [13], might be appropriate to further confirm this discovery.

In summary, we showed that pretreatment with alamandine was able to reduce neutrophil degranulation *in vitro*. *In vivo*, alamandine treatment did not affect macrophage- or Th-cell-mediated inflammation, but impacted on systemic and intraplaque proteases of potential neutrophil origin. These anti-

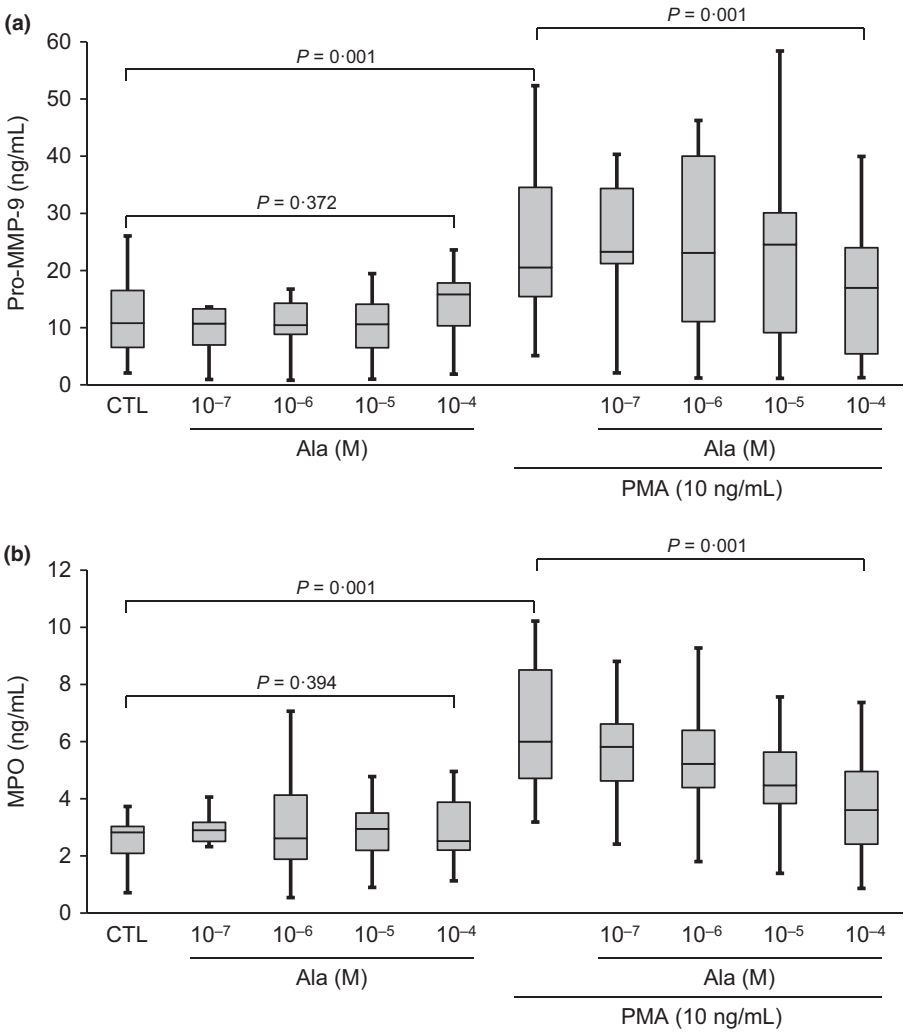

Figure 6 Alamandine abrogates phorbol-12-myristate-13-acetate (PMA)-induced mouse neutrophil degranulation *in vitro*. Mouse neutrophils were preincubated for 60 min in the presence or absence of a control medium (CTL) or different concentrations of alamandine ([Ala], 1×10^{-7} to 1×10^{-4} M). Then, a control medium or 10 ng/mL PMA (positive control) was added for an additional 30 min. Cell supernatants harvested and tested for Pro-MMP-9 (a) and MPO (b) levels. Data are expressed as median (interquartile range), $n = 14$.

inflammatory effects were not accompanied by a protective increase in plaque-stabilizing components (such as collagen), thus suggesting potential concomitant *in vivo* adverse effects. Additional studies are needed to clarify all the therapeutic potential of this agonist of MrgD in atherogenesis.

Acknowledgements

A.R. da Silva is recipient of a grant fellow of CAPES Foundation, Ministry of Education of Brazil. This work was supported by Swiss National Science Foundation Grant to Dr. F. Montecucco (#310030_152639/1). Special gratitude is expressed to Aliki Buhayer (Prism Scientific Sàrl) for medical writing support.

Conflict of interest

The authors all declare that no conflict of interest exists.

Address

Division of Cardiology, Foundation for Medical Researches, Department of Medical Specialties, University of Geneva, 64 avenue de la Roseraie, 1211 Geneva, Switzerland (A. R. Da Silva, S. Lenglet, F. Burger, A. Roth, F. Mach); First Clinic of Internal Medicine, Department of Internal Medicine, University of Genoa School of Medicine, 6 viale Benedetto XV, 16132 Genoa, Italy (F. Carbone, L. Liberale, A. Bonaventura, F. Dallegri, F. Montecucco); IRCCS AOU San Martino – IST, 10 Largo Benzi, 16132 Genoa, Italy (F. Dallegri, F. Montecucco); Institute of Bioengineering, Ecole Polytechnique Fédérale de Lausanne, Route Cantonale, 1015 Lausanne, Switzerland (N. Stergiopulos, R. A. Fraga-Silva); Department of Physiology and Biophysics, Federal University of Minas Gerais, Belo Horizonte, Minas Gerais, Brazil (R. A. S. Santos); Centre of

Excellence for Biomedical Research (CEBR), University of Genoa, 9 viale Benedetto XV, 16132 Genoa, Italy (F. Montecucco).

Correspondence to: Dr Fabrizio Montecucco, First Clinic of Internal Medicine, Department of Internal Medicine, University of Genoa, 6 viale Benedetto XV, 16132 Genoa, Italy. Tel.: +39 010 353 86 94; fax: +39 010 353 86 86; e-mail: fabrizio.montecucco@unige.it

Received 12 August 2016; accepted 1 December 2016

References

1 Carbone F, Mach F, Montecucco F. Update on the role of neutrophils in atherosclerotic plaque vulnerability. *Curr Drug Targets* 2015;**16**:321–33.
2 Carbone F, Nencioni A, Mach F, Vuilleumier N, Montecucco F. Pathophysiological role of neutrophils in acute myocardial infarction. *Thromb Haemost* 2013;**110**:501–14.
3 Nencioni A, da Silva RF, Fraga-Silva RA, Steffens S, Fabre M, Bauer I *et al.* Nicotinamide phosphoribosyltransferase inhibition reduces intraplaque CXCL1 production and associated neutrophil infiltration in atherosclerotic mice. *Thromb Haemost* 2014;**111**:308–22.
4 Döring Y, Drechsler M, Soehnlein O, Weber C. Neutrophils in atherosclerosis: from mice to man. *Arterioscler Thromb Vasc Biol* 2015;**35**:288–95.
5 Montecucco F, Bondarenko AI, Lenglet S, Burger F, Piscitelli F, Carbone F *et al.* Treatment with the GPR55 antagonist CID16020046 increases neutrophil activation in mouse atherogenesis. *Thromb Haemost* 2016;**116**:987–97.
6 Montecucco F, Lenglet S, Gayet-Ageron A, Bertolotto M, Pelli G, Palombo D *et al.* Systemic and intraplaque mediators of inflammation are increased in patients symptomatic for ischemic stroke. *Stroke* 2010;**41**:1394–404.
7 Chu Y, Wilson K, Gu H, Wegman-Points L, Dooley SA, Pierce GL *et al.* Myeloperoxidase is increased in human cerebral aneurysms and increases formation and rupture of cerebral aneurysms in mice. *Stroke* 2015;**46**:1651–6.
8 Lenglet S, Mach F, Montecucco F. Role of matrix metalloproteinase-8 in atherosclerosis. *Mediators Inflamm* 2013;**2013**:659282.
9 Lenglet S, Thomas A, Soehnlein O, Montecucco F, Burger F, Pelli G *et al.* Fatty acid amide hydrolase deficiency enhances intraplaque neutrophil recruitment in atherosclerotic mice. *Arterioscler Thromb Vasc Biol* 2013;**33**:215–23.
10 Kurihara T, Shimizu-Hirota R, Shimoda M, Adachi T, Shimizu H, Weiss SJ *et al.* Neutrophil-derived matrix metalloproteinase 9 triggers acute aortic dissection. *Circulation* 2012;**126**:3070–80.
11 Fraga-Silva RA, Savergnini SQ, Montecucco F, Nencioni A, Caffa I, Soncini D *et al.* Treatment with angiotensin-(1-7) reduces inflammation in carotid atherosclerotic plaques. *Thromb Haemost* 2014;**111**:736–47.
12 da Silva AR, Fraga-Silva RA, Stergiopulos N, Montecucco F, Mach F. Update on the role of angiotensin in the pathophysiology of coronary atherothrombosis. *Eur J Clin Invest* 2015;**45**:274–87.
13 Lautner RQ, Villela DC, Fraga-Silva RA, Silva N, Verano-Braga T, Costa-Fraga F *et al.* Discovery and characterization of alamandine: a novel component of the renin-angiotensin system. *Circ Res* 2013;**112**:1104–11.
14 Montecucco F, Di Marzo V, da Silva RF, Vuilleumier N, Capettini L, Lenglet S *et al.* The activation of the cannabinoid receptor type 2 reduces neutrophilic protease-mediated vulnerability in atherosclerotic plaques. *Eur Heart J* 2012;**33**:846–56.
15 Cheng C, Tempel D, van Haperen R, van der Baan A, Grosveld F, Daemen MJ *et al.* Atherosclerotic lesion size and vulnerability are determined by patterns of fluid shear stress. *Circulation* 2006;**113**:2744–53.
16 Copin JC, da Silva RF, Fraga-Silva RA, Capettini L, Quintao S, Lenglet S *et al.* Treatment with evasin-3 reduces atherosclerotic vulnerability for ischemic stroke, but not brain injury in mice. *J Cereb Blood Flow Metab* 2013;**33**:490–8.
17 Carbone F, Crowe LA, Roth A, Burger F, Lenglet S, Braunersreuther V *et al.* Treatment with anti-RANKL antibody reduces infarct size and attenuates dysfunction impacting on neutrophil-mediated injury. *J Mol Cell Cardiol* 2016;**94**:82–94.
18 Oliveira-Lima OC, Pinto MC, Duchene J, Qadri F, Souza LL, Alenina N *et al.* Mas receptor deficiency exacerbates lipopolysaccharide-induced cerebral and systemic inflammation in mice. *Immunobiology* 2015;**220**:1311–21.
19 Wagenaar GT, Laghmani el H, Fidder M, Sengers RM, de Visser YP, de Vries L *et al.* Agonists of MAS oncogene and angiotensin II type 2 receptors attenuate cardiopulmonary disease in rats with neonatal hyperoxia-induced lung injury. *Am J Physiol Lung Cell Mol Physiol* 2013;**305**:L341–51.
20 Klein N, Gembardt F, Supé S, Kaestle SM, Nickles H, Erfinanda L *et al.* Angiotensin-(1-7) protects from experimental acute lung injury. *Crit Care Med* 2013;**41**:e334–43.
21 van der Vorst EP, Jeurissen M, Wolfs IM, Keijbeck A, Theodorou K, Wijnands E *et al.* Myeloid A disintegrin and metalloproteinase domain 10 deficiency modulates atherosclerotic plaque composition by shifting the balance from inflammation toward fibrosis. *Am J Pathol* 2015;**185**:1145–55.
22 Li B, Zhao Y, Liu H, Meng B, Wang J, Qi T *et al.* Visfatin destabilizes atherosclerotic plaques in apolipoprotein E-deficient mice. *PLoS One* 2016;**11**:e0148273.
23 Karakas M, Koenig W. Myeloperoxidase production by macrophage and risk of atherosclerosis. *Curr Atheroscler Rep* 2012;**14**:277–83.

